Mechanistic insights of 2,4-D sorption onto biochar: Influence of feedstock materials and biochar properties

Sanchita Mandal, Binoy Sarkar, Avanthi Deshani Igalavithana, Yong Sik Ok, Xiao Yang, Enzo Lombi, Nanthi Bolan

PII: S0960-8524(17)31186-0
DOI: http://dx.doi.org/10.1016/j.biortech.2017.07.073
Reference: BITE 18493

To appear in: *Bioresource Technology*

Received Date: 30 May 2017
Revised Date: 12 July 2017
Accepted Date: 13 July 2017

Please cite this article as: Mandal, S., Sarkar, B., Igalavithana, A.D., Ok, Y.S., Yang, X., Lombi, E., Bolan, N., Mechanistic insights of 2,4-D sorption onto biochar: Influence of feedstock materials and biochar properties, *Bioresource Technology* (2017), doi: http://dx.doi.org/10.1016/j.biortech.2017.07.073

Mechanistic insights of 2,4-D sorption onto biochar: Influence of feedstock materials and biochar properties

Sanchita Mandal[1], Binoy Sarkar[1,2], Avanthi Deshani Igalavithana[3], Yong Sik Ok[3,6], Xiao Yang[3], Enzo Lombi[1], and Nanthi Bolan[4,5*]

[1]Future Industries Institute (FII), University of South Australia, Mawson Lakes, SA 5095, Australia,

[2]Department of Animal and Plant Sciences, The University of Sheffield, Sheffield, S10 2 TN, UK

[3]Korea Biochar Research Center, Kangwon National University, Chuncheon 24341, Korea

[4]Cooperative Research Centre for Contaminant Assessment and Remediation of the Environment (CRC CARE), Mawson Lakes, SA 5095, Australia

[5]Global Center for Environmental Remediation, University of Newcastle, Callaghan, NSW 2308, Australia

[6]O-Jeong Eco-Resilience Institute (OJERI) & Division of Environmental Science and Ecological Engineering, Korea University, Seoul, Korea

[*]Corresponding author

Prof Nanthi Bolan

University of Newcastle

Email: Nanthi.Bolan@newcastle.edu.au

Tel: +61 2 49138750

Abstract

Objective of this study was to investigate the mechanisms of 2,4-dichlorophynoxy acetic acid (2,4-D) sorption on biochar in aqueous solutions. Sorption isotherm, kinetics, and desorption experiments were performed to identify the role of biochars' feedstock and production conditions on 2,4-D sorption. Biochars were prepared from various green wastes (tea, burcucumber, and hardwood) at two pyrolytic temperatures (400 and 700˚C). The tea waste biochar produced at 700 ˚C was further activated with steam under a controlled flow. The sorption of 2,4-D was strongly dependent on the biochar properties such as specific surface area, surface functional groups, and microporosity. The steam activated biochar produced from tea waste showed the highest (58.8 mg g^{-1}) 2,4-D sorption capacity, which was attributed to the high specific surface area (576 m^2g^{-1}). The mechanism of 2,4-D removal from aqueous solution by biochar is mainly attributed to the formation of heterogeneous sorption sites due to the steam activation.

Keywords: 2,4-D, biochar, Pyrolysis, Physical activation, Sorption kinetics

1. Introduction

Agriculture activities, forestry, and maintenance of green spaces rely heavily on the use of herbicide to control weeds. The leaching and runoff from agricultural and forest land, deposition from the aerial application, and discharge of industrial wastewater to ground and surface water bodies have caused severe contamination of the environment by herbicides. Many herbicides are not easily biodegradable, and some are carcinogenic in

nature, and as such represent a concerning source of environmental toxicant (Gupta et al., 2006).

2,4-dichlorophenoxy acetic acid (2,4-D) is one of the oldest and more widely used herbicides (Kearns et al., 2014). 2,4-D is a systemic herbicide widely employed to selectively control broadleaf weeds. According to world health organization (WHO), 2,4-D is categorized as a substance of "possibly carcinogenic to humans" (Loomis et al., 2015). It is highly soluble in water (solubility 900 mg L^{-1}) in comparison to other organic micro-pollutants (e.g. pharmaceuticals and hydrocarbons). The p*Ka* value of the herbicide is 2.7. Due to these reasons, removing 2,4-D from polluted waters can be challenging. The herbicide is anionic in nature, which also makes it weakly retained by intrinsically negatively charged soil and subsurface particles (Hermosin et al., 2006). This enables 2,4-D to quickly reach to the groundwater which, in many countries, is a common source of drinking water.

The development of an efficient, easily accessible and inexpensive technology is required for the removal of 2,4-D and other anionic herbicide compounds from water. The application of locally generated and low-cost adsorbents in water treatment processes can be a possible solution to address this issue, especially for developing countries.

Carbon (C) based biomass such as biochar has been used extensively to reduce toxicity levels of different pollutants in the environment (Ahmad et al., 2014; Uchimiya et al., 2010). Biochar is a by-product of the thermal decomposition of various organic biomasses to produce bio-oil. This process occurs over a range of temperatures (200-800 ˚C) under nitrogen environment with a limited supply of oxygen (Lehmann & Joseph, 2009). In the recent years, biochar has created a broad research interests due to

its surface properties, high surface area, pore volume, and pore diameter that make it a strong candidate for the removal of contaminants from soil and water bodies (Mandal et al., 2016). Furthermore, biochar has a range of oxygen-containing surface functional groups (e.g., carboxyl, phenolic, hydroxyls) which make this C-based material effective to interact with diverse types of environmental contaminants (Lehmann & Joseph, 2015).

However, biochar properties (surface area, pore size distribution, surface charge and functional groups) greatly depend on different parameters such as biomass sources, pyrolysis temperature, pyrolysis procedure and post-treatment processes of the product (Lehmann, 2007b; Lehmann et al., 2011). From an environmental protection perspective, enhanced contaminant retention capacity, faster removal/sorption kinetics and low reversibility of the sorption process are the most desirable characteristics of biochar materials.

Previous studies investigated the prevention of herbicide mobility in the environment through biochar application. For example, Kearns et al. (2014) found that biochar prepared from woodchips (350-700 ˚C), bamboo (500-700 ˚C) and corncobs (600 ˚C) adsorbed a higher quantity of 2,4-D compared to a commercial activated carbon. Similarly, Lü et al. (2012) reported that biochar produced from rice straw at 350 ˚C reduced the mobile 2,4-D concentration (100-600 µmol L^{-1}) in soils by up to 45%. In their study Lü et al. (2012) also investigated the effect of different pyrolysis temperatures (200, 350 and 500 ˚C) on biochar pore properties, surface functional groups and the herbicide sorption capacity.

The current study hypothesized that the presence of a greater surface area due to the presence of microporous structure and aromaticity or functional groups like carbonyl C=O, hydroxyl O-H and carboxyl in biochar would increase its ability to adsorb 2,4-D from aqueous solutions. In addition to the study of Lü et al. (2012) reported above there are a few other studies available on the sorption of 2,4-D by biochar (Gupta et al., 2006; Kearns et al., 2014), but none of these reports has specifically focused on a systematic investigation of the effect of feedstock source and steam activation on biochar's characteristics and their role on 2,4-D sorption. Steam activation is included in this study as it has been reported that this process can increase the degree of microporosity in biochar (Downie et al., 2009). This study underpins the feasibility of using biochar for remediating of 2,4-D and other problematic pesticides.

2. Materials and methods

2.1. Reagents

2,4-D (Sigma-Aldrich, Australia) was dissolved in ultrapure water to prepare a 1000 mg L^{-1} stock solution. The pH of the stock solution was raised to 11 by dropwise addition of 1 N sodium hydroxide (NaOH) to enhance the compound's solubility (Kearns et al., 2014). The stock solution was then stored in a dark container in a cold room (4 ^{o}C) for further use. The stock solution was diluted in 20 mM phosphate buffer saline (PBS) at pH 7 to get the targeted initial 2,4-D concentration of 100 mg L^{-1} for the kinetic sorption experiments. Similarly, six working solutions of 2,4-D (10, 50, 100, 200, 400, and 500 mg L^{-1}) were also prepared in PBS for conducting the sorption isotherm experiments.

117 **2.2. Biochar preparation**

118 Four different types of feedstock were used to prepare biochar in this study. They were
119 tea waste, burcucumber, oak wood and bamboo. Tea waste was collected from a tea
120 factory after tea leaf processing and washed several times in distilled to remove
121 impurities. After washing the material was air-dried, crushed and ground to <1 mm in
122 particle size for biochar preparation. Tea wastes were pyrolyzed at 700 ˚C with a
123 heating rate of 7 ˚C min^{-1} for 2 h using a modified N11/H Nabertherm (Germany)
124 furnace (Ahmad et al., 2012; Rajapaksha et al., 2014). Nitrogen flow rate was set to 5
125 mL min^{-1} throughout the pyrolyzation. For steam activation, samples were treated with
126 5 mL min^{-1} of steam during the last 45 min of the 2 h total holding time at the peak
127 temperature (700 ˚C). After steam activation, samples were allowed to cool inside the
128 chamber to 30 ˚C and then the final weight was recorded. The samples from tea waste
129 with and without steam activation were termed as TW-BC and TW-BCS, respectively.
130 Burcucumber (*Cucumis anguria*) plants were collected and dried in air, then in an oven
131 at 60 ˚C for 24 h. After drying, samples were ground and passed through <1 mm sieve.
132 Crushed samples were pyrolyzed at 700℃ by following the same pyrolysis procedure
133 used for tea waste. This biochar was termed as burcucumber biochar (BU-BC).
134 Oakwood and bamboo feedstock were collected and pyrolyzed at 400 ˚C for 2 h using a
135 muffle furnace. Heating rate and N_2 supply were as above. After pyrolyzation, produced
136 biochars were termed as OW-BC and B-BC.
137

138 **2.3. Surface characterization of biochar**

139 The pH of the biochar samples was measured using a pH meter (smartCHEM-LAB
140 Laboratory Analyzer) in deionized water (1:10 ratio, W/V) after agitation in the end

over end shaker at 20 rpm for 2 h followed by 5 min of settling time. The electrical conductivity (EC) of biochars was also measured in the same suspension using an EC electrode (smartCHEM-LAB Laboratory Analyzer) following 12 h of sediment settling. The C and N contents of biochar samples were determined with a Leco TruMac CNS Analyzer (LECO Corporation, USA). Cation exchange capacity (CEC) of the biochar samples was measured using the method described by Zelazny et al. (1996).

Biochar surface functional groups were determined using a Fourier-transform infrared spectrometer (FT-IR; Frontier, PerkinElmer, UK) at the wavenumber range of 600 - 4000 cm^{-1} by potassium bromide (KBr) pellet method. Each pellet was scanned 32 times at the resolution of 0.4 cm^{-1}. Baseline corrected spectra were used to identify the representative peaks of functional groups based on published literature (software; Thermo Nicolet). X-ray photoelectron spectroscopy (XPS) analysis was performed using a XPS spectrometer (K-Alpha, Thermo Scientific, UK) with a monochromatic Al α-Alpha radiation source, and a spot size around 400 μm in diameter with a detection limit around 0.5-1.0%. Gaussian-Lorentzian sum function was used for the XPS spectra deconvolution by XPSPEAK41.

Biochar particles were also examined by field emission scanning electron microscope (FE-SEM; Hitachi S-4300, Japan) to identify the surface morphology. The specific surface area and pore volume were analyzed by the Brunauer–Emmett–Teller (BET) method at −196 °C using a Gemini 2380 Surface Area Analyzer. Pore diameter was further determined using a gas sorption analyzer (NOVA-1200; Quantachrome Corp., Boynton Beach, FL, USA) (Ahmad et al., 2014).

165 **2.4. 2,4-D sorption kinetics and isotherm**

166 2,4-D sorption experiments were performed using a batch equilibrium method. The
167 kinetic experiment was conducted in 250 mL Schott bottle by mixing 0.25 g of each
168 biochar sample with 100 mL of 100 mg L^{-1} 2,4-D solution (in PBS). All the containers
169 were wrapped with aluminum foil to maintain in darkness. The mixture was then
170 agitated using an end-over-end shaker at room temperature (23 ± 1 ˚C) at 10 rpm for 72
171 h. Subsamples (2 mL) were taken from each bottle at different time intervals (0.25, 0.5,
172 1, 2, 3, 5, 7, 10, 16, 24, 36, 48, 60, and 72 h). Samples were filtered using 0.45 µm
173 cellulose ester filters immediately after collection. The filtrates after appropriate dilution
174 were analyzed to determine 2,4-D concentrations by a spectrophotometric method at
175 282 nm (Aksu & Kabasakal, 2004) on a UV-VIS-NIR-Spectrophotometer (UV-3600,
176 Shimadzu, Japan).
177 Sorption isotherms were determined at a constant pH 7 maintained by using PBS. It was
178 found that the PBS was sufficient to control pH within ±0.2 units after addition of
179 biochar materials (Kearns et al., 2014). Six working solutions (10, 50, 100, 200, 400,
180 and 500 mg L^{-1}) of 2,4-D were prepared as described above. Fifty mL centrifuge tubes
181 were used for the isotherm experiment. The weights of tubes and lids were recorded
182 before adding biochar and 2,4-D solutions, which was needed to calculate the entrapped
183 liquid weight and associated 2,4-D concentration during desorption experiments as
184 explained later. Exactly 0.05 g of each biochar sample was placed inside the centrifuge
185 tube, and 20 mL of each of the 2,4-D working solutions was added to it. The samples
186 were agitated at 10 rpm using an end-over-end shaker for 72 h at room temperature
187 (23±1 ˚C). The equilibration time was decided from the sorption kinetic experiments.
188 After equilibration samples were centrifuged at 2403-G for 15 min to get clear

189 supernatants which were further filtered using 0.45 µm cellulose ester filters. The
190 concentration of 2,4-D in the aliquot was determined by a UV-VIS-NIR-
191 Spectrophotometer as explained earlier.
192 After removing the supernatant, the weight of tubes containing wet biochar sediments
193 was recorded (for calculating the entrapped liquid weight). All the sorption experiments
194 were conducted in duplicates. The labware used in this study did not sorb any 2,4-D.
195 To evaluate and compare the 2,4-D sorption capacity of different biochars, the
196 experimental data were fitted using both Freundlich and Langmuir sorption models. The
197 respective mathematical expressions of these models are provided as Supplementary
198 Information (SI).
199 Similarly, the sorption kinetic data were fitted to various kinetic models such as
200 parabolic diffusion, elovich equation, pseudo-first order and pseudo-second order
201 models. The mathematical expressions of these models are also given in SI.
202
203 **2.5. 2,4-D desorption**
204 The desorption of 2,4-D was determined following sorption of a known volume and
205 concentration of the 2,4-D solution. Just after the sorption experiment, 20 mL deionized
206 water was added to the sediment in each tube. Samples were agitated at 10 rpm on an
207 end-over-end shaker for 24 h at room temperature (23±1 ˚C). The suspension was then
208 centrifuged at 2403-G for 15 min. Clear supernatants were further filtered using 0.45
209 µm cellulose ester filter for 2,4-D analysis as stated above. The amount of 2,4-D which
210 was entrapped in the wet biochar sediment coming straight from the sorption
211 experiment was taken into consideration for calculating the respective desorption
212 amount.

2.6. Statistical analysis

An analysis of variance (ANOVA) using SPSS software packages (IBM SPSS Statistics 23) was performed on the data to analyze the 2,4-D sorption capacity of different biochar samples. A post hoc t-test at 5% level of significance was also conducted to quantify the significance difference between biochar samples. Variability of the data was expressed as the standard deviation (STDEV) and a p value of <0.05 was considered as statistically significant.

3. Results and discussion

3.1. Characterization of biochar samples

The key physicochemical characteristics of biochar samples are shown in Table 1. Biochar prepared from tea waste with steam activation (TW-BCS) had a higher pH (11.9) and CEC (15.9 $cmol_c\ kg^{-1}$) values compared to the other four biochars. Furthermore, BU-BC showed a higher EC value (1403 $\mu S\ m^{-1}$) than other biochars (Table 1).

[Table 1]

The BU-BC had a much lower surface area (2.3 $m^2\ g^{-1}$; pore volume: 0.008 $cm^3 g^{-1}$) than all the other materials probably due to the lower volatile organic matter content in the burcucumber biomass than the other biomass. For example, the C content of BU-BC was very low compared to TW-BCS produced at the same temperature (Table 1). The BU-BC contains a high amount of mineral ash which does not produce a high surface area as organic material (Lehmann, 2007a). Even though feedstock characteristics is important, pyrolysis temperature also seems to have a prominent effect on the surface

area of the products. For example, TW-BCS had an extremely high surface area and pore volume (576 m^2g^{-1}; 109 cm^3kg^{-1}) compared to TW-BC and biochars from other two sources. Ahmad et al. (2012) reported that biochar produced at 700 ˚C had much higher surface area than that produced at a lower temperature 300 ˚C, which reflects the temperature effect on opening up of pore spaces due to the removal of volatile organic matters. Another study by Kloss et al. (2012) also found that increasing temperature from 400 to 525 ˚C increased the surface area of wheat straw-derived biochar from 4.8 to 14.2 m^2g^{-1}.

Biochar usually contains a microporous structure with higher pore volume and defined pore diameter. It was observed in this study that the pore volume of steam activated tea-waste biochar was the highest (109 $cm^3\,kg^{-1}$) compared to the non-activated biochar and products produced from other biomass sources. Azargohar and Dalai (2008) also found that the physical (steam) activation increased the total pore volume of biochar samples. Similarly, an increase in the pore diameter of the biochar samples was observed as a result of steam activation (Table 1). Steam activated biochar with a large number of micropores (0-2 nm), and pore volume as shown in Table 1 could thus provide an increased herbicide sorption capacity as compared to the non-activated product (Rajapaksha et al., 2016; Rajapaksha et al., 2014). The polar surface area of 2,4-D is 47 $Å^2$. The relationship between pore size/diameter and 2,4-D sorption was investigated in the previous study by Kearns et al. (2014). The authors reported that pyrolysis conditions that produced BET surface areas up to 400 m^2g^{-1} primarily generated micropores accessible to N_2, but not 2,4-D due to the size exclusion. However, pyrolysis conditions that produced surface areas between 400 to 600 m^2g^{-1} increased 2,4-D sorption with increasing surface area, indicating the progressive widening of micropores

into the larger sized pores that accommodated 2,4-D molecules. In our study, we also found the increased surface area and pore diameter with steam activation of tea waste biochar. Moreover, these properties increased 2,4-D sorption by steam-activated biochar.

Biochars produced at the higher temperature were highly carbonized and exhibited highly aromatic structures, which was shown by the FTIR data. The IR spectra showed the presence of C-H, C=O, carboxyl, phenolic and other oxygen-containing functional groups on biochar surfaces (Supplementary information).

The bands observed at 3446 cm^{-1} (TW-BC and TW-BCS) can be assigned to the hydroxyl (-OH) stretching vibration (Yaman, 2004). The hydroxyl groups might be decreased with steam activation due to the ignition loss of OH during the activation at high temperature (Yuan et al., 2011). Bands at 1567 and 1557 cm^{-1} represented the presence of strong nitro (N-O) stretching vibration (Nakanishi, 1962). The presence of C=C and carbonyl (-COH) was observed at 1432 and 1431 cm^{-1}, and the intensity of these groups was increased after steam activation of the biochar (Hsu et al., 2009). The increased band intensity at 1384 cm^{-1} represented the presence of –COOH bending vibration in the steam activated biochar (Supplementary information). Bands at 874 and 875 cm^{-1} can be assigned to the aromatic C-H bending (Uchimiya et al., 2013) (Supplementary information). However, FTIR spectra did not show very significant differences between TW-BC and TW-BCS except demonstrating changes in the intensity of certain bands.

While FTIR data represented the bulk surface characteristics of biochar materials, XPS analysis aimed to identify the presence of specific functional groups, especially the O-containing functional groups. The O1s and C1s spectra of TW-BC and TW-BCS are

presented in Fig. 1. The relative percentage of specific functional groups from O1s and C1s spectra are shown in the supplementary section. The XPS spectra showed that the O content of the steam-activated biochar (TW-BCS; O atom % = 21.04) was higher than the non-activated biochar (TW-BC; O atom % = 17.47). The peaks at binding energies of 531.3 and 531.9 eV were assigned to O=C and O-C functional groups. The relative intensity of O=C and O-C functional groups are significantly higher in TW-BCS (15.6 and 73.7%) compared to TW-BC (14.4 and 59.2%) (Fig. 1a and 1b). Moreover, the relative intensity of –COOH functional groups at a binding energy of 289.3 eV is only observed in TW-BCS (Fig. 1c and 1d; Supplementary information) (Liu et al., 2010). The XPS results confirmed that the steam activation could conserve a greater proportion of O-containing functional groups (e.g., –COOH as also indicated by FTIR spectra) when compared with the non-activated biochar prepared from the same feedstock.

[Figure 1]

The difference between CEC values also described the presence of effective functional groups on biochar surfaces. Previous studies found that increasing pyrolysis temperature decreased the CEC value due to the loss of carboxyl functional groups during the pyrolysis process (Gai et al., 2014). However, the current study demonstrated that the steam activated biochar had the highest CEC value in comparison to other products (Table 1). Therefore, biochars produced at a similar temperature but with steam activation might help to conserve the oxygen-containing functional groups (like carboxyl), which would lead to a higher CEC value. Harvey et al. (2011) also reported that the higher CEC value of biochar might reflect the presence of a higher carboxylic group contents.

Scanning Electron Microscopic (SEM) images showed the morphological and structural changes between TW-BC and TW-BCS (Supplementary information). High-resolution SEM images (2000x) depicted more defined pore structure in TW-BCS compared to TW-BC. The well-defined pore structure might have caused the greater surface area in the steam activated biochar than the non-activated product (Azargohar & Dalai, 2008) (Table 1).

3.2. Sorption of 2,4-D by biochar

3.2.1. . 2,4-D sorption kinetics

Several kinetic models such as parabolic diffusion, elovich equation, pseudo-first order and pseudo-second order models were tested in this study. The best kinetic model fitting was determined by considering the estimated correlation coefficient (R^2) values, which was highest for the pseudo-second order model (Table 2). Yao et al. (2011) found that the pseudo-first order and second order models better described the phosphate removal data on biochar compared to the elovich equation. All the other model parameters presented in the supplementary information.

The sorption kinetic modeling allowed to calculate the sorption rate as well as explained the possible reaction mechanisms by identifying suitable rate expression characteristics. The sorption rate of 2,4-D was initially fast and then followed a slower sorption rate until gradually approaching an equilibrium (Fig. 2). The initial faster sorption might attribute to a large amount of pore spaces available for the sorption (Rajapaksha et al., 2016). The steam activated biochar adsorbed 2,4-D more efficiently compared to the other products (Fig. 2). The reason could be that the steam activation enhanced the pore volume and pore diameter (Table 1) of biochar samples, which influenced the sorption

process. Previous studies also found similar results, for example, Lima et al. (2010) reported that steam activation could increase the sorption ability of biochar by enhancing the pore diameter. Rajapaksha et al. (2016) found that steam activation of biochar could increase the pore size from 1.75 to 1.99 nm, which consequently increased sulfamethazine sorption by the product.

[Figure 2]

The estimated kinetic parameters for the pseudo-second order model are shown in Table 2 and the parameters for the other models in supplementary information. The pseudo-first order model could be more relevant when the initial adsorbate concentration was higher, and the pseudo-second order model could be more applicable when the initial adsorbate concentration was lower (Liu, 2008). The best-fitted pseudo-second order model in the current study suggested that the sorption of 2,4-D on biochar was a function of the availability of surface sorption sites (Zhang et al., 2012). Furthermore, the best fitness of pseudo-second order model for 2,4-D sorption on biochar confirms that the sorption process may be controlled by both the physical and chemical processes (Sarkar et al., 2010). The pseudo-second order rate constant was increased from 0.04 in TW-BC to 0.21 in TW-BCS (Table 2). The K (sorption constant) value for TW-BCS was higher than for the rest of the four biochars (Table 2). This indicated that the sorption of 2,4-D on steam activated biochar was faster than the non-activated product and biochar from other sources. The kinetic sorption results of 2,4-D on biochar indicated that the feedstock composition and steam activation played a key role in the sorption process. The kinetics of sorption of the biochars followed the similar order of 2,4-D sorption capacities obtained from the sorption isotherm calculations (section

3.2.2). The difference in sorption ability could greatly depend on the biochar characteristics which are a function of biomass source and production technology (Martin et al., 2012). In this study, biochar prepared at the same temperature but with steam activation enhanced the specific characteristics (surface area, pore diameter, functional groups, pH) of biochar, which led to an increased 2,4-D sorption capacity. [Table 2]

3.2.2. *2,4-D sorption isotherm*

Two isothermal models such as Freundlich and Langmuir were tested to fit the sorption data. The Freundlich model best described the data with R^2 values of up to 0.98 (Table 3). Zhang et al. (2011) found that the sorption of simazine on biochar was best fitted to the Freundlich isotherm model with high R^2 (>0.98) values. The lower n value from the Freundlich model indicated the heterogeneous sorption domain in the sorbent and the presence of higher sorption site energy distribution (Pignatello & Xing, 1995). The fitting parameters for all attempted models are shown in the supplementary information. [Figure 3]

Fig. 3 represents the Freundlich isotherms for the sorption of 2,4-D to five biochar samples. The steam activated biochar had the highest sorption capacity (58.8 mg g^{-1}) with moderate n and high K and R^2 values, compared to the other four biochars. The best 2,4-D sorption fitness with Freundlich model compared to Langmuir model suggests the formation of more heterogeneous sorption sites on biochar because of the steam activation (Rusmin et al., 2015). In general, 2,4-D sorption capacity decreased in the order: TW-BCS>OW-BC>BU-BC>B-BC>TW-BC. For TW-BC and TW-BCS, some nonlinearity was observed at low adsorbate concentration, but the linearity

increased with increasing 2,4-D concentrations. The high sorption on TW-BCS might be attributed to the high surface area of the biochar. Previous studies also supported our findings, for example, Ahmad et al. (2012) observed that biochar prepared at a higher temperature with high surface area (448.2 m^2 g^{-1}) removed trichloroethylene (TCE) more efficiently than that prepared at a lower temperature (300 ˚C; surface area: 3.14 m^2 g^{-1}). Few authors also found that biochar with a lower surface area could adsorb more 2,4-D than biochar with a higher surface area. For example, Lü et al. (2012) found that biochar produced from rice straw at 300 ˚C (20.6 m^2g^{-1}) could adsorb 2,4-D more than biochar at 500 ˚C (128 m^2g^{-1}). The reason could be the difference in the chemical composition between the biochar samples which played an important role in increasing the sorption capacity at low temperature despite having a lower surface area (Lü et al., 2012).

In order to better compare the sorption ability of biochar to those of other sorbents, the sorption distribution coefficient (K_d) was calculated (Table 4). The K_d values were normalized to organic carbon content (K_{oc}). The formula for K_d and K_{oc} is presented in the supplementary information. Within the tested concentration ranges, the K_d value was on the order of 10^3 (L kg^{-1}) for TW-BCS. The observed K_d values are much larger than those reported in the previous studies for natural geo-sorbents, including soils (K_d<10 L kg^{-1}), humic substances, and clay minerals (K_d<100 L kg^{-1}) (Ji et al., 2009) and less than those recorded for black carbon (K_d<10^6 L kg^{-1}) (Teixidó et al., 2011). The K_d values of 2,4-D by TW-BCS was significantly higher than biochar produced from other sources. Also, the sorption studies showed a higher 2,4-D removal by TW-BCS than other biochar samples. The reason could be attributed to the microporous nature, higher surface area and aromatic carbon structure of the TW-BCS materials. Our

findings are supported by previous research, such as Ren et al. (2016) found that the sorption affinity of phenanthrene to biochar (700 ˚C) was significantly higher than biochar (300 ˚C) because of microporous nature and higher surface area of biochar (700 ˚C). Moreover, from Table 4 the increased K_{oc} value for TW-BCS was also observed. K_{oc} values are useful to estimate the relative affinity and attraction of the herbicide to the biochar materials. Therefore, it also predicts the herbicide mobility in the solution (Futch & Singh, 1999). Higher K_{oc} values correlate with the greater sorption of 2,4-D by biochar samples whereas lower K_{oc} values represent the higher mobility of 2,4-D in solution (Buttler et al., 1991). Therefore, sorption of 2,4-D to steam activated biochar was much higher compared to non-activated biochar due to having improved surface properties.

[Table 3]

[Table 4]

3.2.3. 2,4-D desorption

The sorbed 2,4-D by a single extraction with deionized water only removed 4.4 to 21.5% of 2,4-D that was sorbed. A maximum 21.5% of 2,4-D desorption was observed in the case of TW-BC, whereas the lowest desorption was observed in the case of TW-BCS (4.4%). This indicated that the steam activated biochar had a stronger binding affinity to 2,4-D compare to other biochars. This also implied that biochar with steam activation held a lesser risk of possible release of adsorbed 2,4-D into the environment. The reason could be the diffusion process that might limit/decrease the desorption of 2,4-D from steam activated biochar (TW-BCS) (Ahmad et al., 2012). Loganathan et al. (2009) observed that the herbicide atrazine remained much higher (five times) in the char-amended soil after desorption and washing steps compared to soil alone.

Desorption of pesticides like carbofuran from biochar prepared from red gum wood (*Eucalyptus* spp.) was also less than the control due to the strong sorption of pesticide on biochar surface (Yu et al., 2009).

4. Conclusions

Results of this research demonstrated that the laboratory prepared biochars could adsorb 2,4-D from solution. Sorption studies showed that the steam activated biochar adsorbed 2,4-D more efficiently than its non-steam activated biochars. Due to having a higher surface area, pore volume, and pore diameter the steam activated biochar showed a higher 2,4-D sorption capacity. Furthermore, a reduced 2,4-D desorption indicated that the steam activated biochar could also retain 2,4 D more efficiently. Future studies should focus more in detail on the mechanism of herbicide sorption and retention of a range of activated biochars in comparison to their conventionally prepared counterparts.

E-supplementary data for this work can be found in e-version of this paper online.

Acknowledgments

Sanchita Mandal is thankful to the Department of Education and Training, Government of Australia, for awarding her an Australian Postgraduate Award (APA).

452 **Reference**

453 1. Ahmad, M., Lee, S.S., Dou, X., Mohan, D., Sung, J.-K., Yang, J.E., Ok, Y.S.
454 2012. Effects of pyrolysis temperature on soybean stover- and peanut shell-
455 derived biochar properties and TCE adsorption in water. *Bioresource*
456 *Technology*, **118**, 536-544.
457 2. Ahmad, M., Rajapaksha, A.U., Lim, J.E., Zhang, M., Bolan, N., Mohan, D.,
458 Vithanage, M., Lee, S.S., Ok, Y.S. 2014. Biochar as a sorbent for contaminant
459 management in soil and water: a review. *Chemosphere*, **99**, 19-33.
460 3. Aksu, Z., Kabasakal, E. 2004. Batch adsorption of 2, 4-dichlorophenoxy-acetic
461 acid (2, 4-D) from aqueous solution by granular activated carbon. *Separation*
462 *and Purification Technology*, **35**(3), 223-240.
463 4. Azargohar, R., Dalai, A.K. 2008. Steam and KOH activation of biochar:
464 Experimental and modeling studies. *Microporous and Mesoporous Materials*,
465 **110**(2–3), 413-421.
466 5. Buttler, T., Hornsby, A., Tucker, D., Knapp, J., Noling, J. 1991. Citrus:
467 managing pesticides for crop production and water quality protection: a
468 supplement to the IFAS pest control guides. *Circular-Florida Cooperative*
469 *Extension Service (USA)*.
470 6. Downie, A., Crosky, A., Munroe, P. 2009. Physical properties of biochar.
471 *Biochar for environmental management: Science and technology*, 13-32.
472 7. Futch, S., Singh, M. 1999. Herbicide mobility using soil leaching columns.
473 *Bulletin of environmental contamination and toxicology*, **62**(5), 520-529.

8. Gai, X., Wang, H., Liu, J., Zhai, L., Liu, S., Ren, T., Liu, H. 2014. Effects of feedstock and pyrolysis temperature on biochar adsorption of ammonium and nitrate. *PloS one*, **9**(12), e113888.
9. Gupta, V.K., Ali, I., Suhas, Saini, V.K. 2006. Adsorption of 2,4-D and carbofuran pesticides using fertilizer and steel industry wastes. *Journal of Colloid and Interface Science*, **299**(2), 556-563.
10. Harvey, O.R., Herbert, B.E., Rhue, R.D., Kuo, L.-J. 2011. Metal interactions at the biochar-water interface: energetics and structure-sorption relationships elucidated by flow adsorption microcalorimetry. *Environmental science & technology*, **45**(13), 5550-5556.
11. Hermosin, M., Celis, R., Facenda, G., Carrizosa, M., Ortega-Calvo, J., Cornejo, J. 2006. Bioavailability of the herbicide 2, 4-D formulated with organoclays. *Soil biology and Biochemistry*, **38**(8), 2117-2124.
12. Hsu, N.-H., Wang, S.-L., Liao, Y.-H., Huang, S.-T., Tzou, Y.-M., Huang, Y.-M. 2009. Removal of hexavalent chromium from acidic aqueous solutions using rice straw-derived carbon. *Journal of hazardous materials*, **171**(1), 1066-1070.
13. Ji, L., Chen, W., Zheng, S., Xu, Z., Zhu, D. 2009. Adsorption of sulfonamide antibiotics to multiwalled carbon nanotubes. *Langmuir*, **25**(19), 11608-11613.
14. Kearns, J.P., Wellborn, L.S., Summers, R.S., Knappe, D.R.U. 2014. 2,4-D adsorption to biochars: Effect of preparation conditions on equilibrium adsorption capacity and comparison with commercial activated carbon literature data. *Water Research*, **62**, 20-28.
15. Kloss, S., Zehetner, F., Dellantonio, A., Hamid, R., Ottner, F., Liedtke, V., Schwanninger, M., Gerzabek, M.H., Soja, G. 2012. Characterization of slow

pyrolysis biochars: effects of feedstocks and pyrolysis temperature on biochar properties. *Journal of environmental quality*, **41**(4), 990-1000.

16. Lehmann, J. 2007a. Bio-energy in the black. *Frontiers in Ecology and the Environment*, **5**(7), 381-387.
17. Lehmann, J. 2007b. A handful of carbon. *Nature*, **447**(7141), 143-144.
18. Lehmann, J., Joseph, S. 2009. *Biochar for environmental management: science and technology*. Earthscan.
19. Lehmann, J., Joseph, S. 2015. *Biochar for environmental management: science, technology and implementation*. Routledge.
20. Lehmann, J., Rillig, M.C., Thies, J., Masiello, C.A., Hockaday, W.C., Crowley, D. 2011. Biochar effects on soil biota - A review. *Soil Biology and Biochemistry*, **43**(9), 1812-1836.
21. Lima, I.M., Boateng, A.A., Klasson, K.T. 2010. Physicochemical and adsorptive properties of fast□pyrolysis bio□chars and their steam activated counterparts. *Journal of chemical technology and biotechnology*, **85**(11), 1515-1521.
22. Liu, S., Sun, J., Huang, Z. 2010. Carbon spheres/activated carbon composite materials with high Cr (VI) adsorption capacity prepared by a hydrothermal method. *Journal of hazardous materials*, **173**(1), 377-383.
23. Liu, Y. 2008. New insights into pseudo-second-order kinetic equation for adsorption. *Colloids and Surfaces A: Physicochemical and Engineering Aspects*, **320**(1), 275-278.
24. Loganathan, V.A., Feng, Y., Sheng, G.D., Clement, T.P. 2009. Crop-residue-derived char influences sorption, desorption and bioavailability of atrazine in soils. *Soil Science Society of America Journal*, **73**(3), 967-974.

25. Loomis, D., Guyton, K., Grosse, Y., El Ghissasi, F., Bouvard, V., Benbrahim-Tallaa, L., Guha, N., Mattock, H., Straif, K., IARC, L. 2015. Carcinogenicity of lindane, DDT, and 2, 4-dichlorophenoxyacetic acid. *The Lancet. Oncology*, **16**(8), 891.

26. Lü, J., Li, J., Li, Y., Chen, B., Bao, Z. 2012. Use of rice straw biochar simultaneously as the sustained release carrier of herbicides and soil amendment for their reduced leaching. *Journal of agricultural and food chemistry*, **60**(26), 6463-6470.

27. Mandal, S., Sarkar, B., Bolan, N., Ok, Y.S., Naidu, R. 2016. Enhancement of chromate reduction in soils by surface modified biochar. *Journal of environmental management*, **186**, 277-284.

28. Martin, S.M., Kookana, R.S., Van Zwieten, L., Krull, E. 2012. Marked changes in herbicide sorption–desorption upon ageing of biochars in soil. *Journal of Hazardous Materials*, **231–232**, 70-78.

29. Nakanishi, K. 1962. Infrared absorption spectroscopy, practical.

30. Pignatello, J.J., Xing, B. 1995. Mechanisms of slow sorption of organic chemicals to natural particles. *Environmental Science & Technology*, **30**(1), 1-11.

31. Rajapaksha, A.U., Vithanage, M., Lee, S.S., Seo, D.-C., Tsang, D.C.W., Ok, Y.S. 2016. Steam activation of biochars facilitates kinetics and pH-resilience of sulfamethazine sorption. *Journal of Soils and Sediments*, **16**(3), 889-895.

32. Rajapaksha, A.U., Vithanage, M., Zhang, M., Ahmad, M., Mohan, D., Chang, S.X., Ok, Y.S. 2014. Pyrolysis condition affected sulfamethazine sorption by tea waste biochars. *Bioresource technology*, **166**, 303-308.

546 33. Ren, X., Yuan, X., Sun, H. 2016. Dynamic changes in atrazine and phenanthrene
547 sorption behaviors during the aging of biochar in soils. *Environmental Science*
548 *and Pollution Research*, 1-10.
549 34. Rusmin, R., Sarkar, B., Liu, Y., McClure, S., Naidu, R. 2015. Structural
550 evolution of chitosan–palygorskite composites and removal of aqueous lead by
551 composite beads. *Applied Surface Science*, **353**, 363-375.
552 35. Sarkar, B., Xi, Y., Megharaj, M., Krishnamurti, G.S.R., Rajarathnam, D., Naidu,
553 R. 2010. Remediation of hexavalent chromium through adsorption by bentonite
554 based Arquad® 2HT-75 organoclays. *Journal of Hazardous Materials*, **183**(1–
555 3), 87-97.
556 36. Teixidó, M., Pignatello, J.J., Beltrán, J.L., Granados, M., Peccia, J. 2011.
557 Speciation of the ionizable antibiotic sulfamethazine on black carbon (biochar).
558 *Environmental science & technology*, **45**(23), 10020-10027.
559 37. Uchimiya, M., Lima, I.M., Thomas Klasson, K., Chang, S., Wartelle, L.H.,
560 Rodgers, J.E. 2010. Immobilization of heavy metal ions (CuII, CdII, NiII, and
561 PbII) by broiler litter-derived biochars in water and soil. *Journal of Agricultural*
562 *and Food Chemistry*, **58**(9), 5538-5544.
563 38. Uchimiya, M., Orlov, A., Ramakrishnan, G., Sistani, K. 2013. In situ and ex situ
564 spectroscopic monitoring of biochar's surface functional groups. *Journal of*
565 *Analytical and Applied Pyrolysis*, **102**, 53-59.
566 39. Vithanage, M., Rajapaksha, A.U., Zhang, M., Thiele-Bruhn, S., Lee, S.S., Ok,
567 Y.S. 2015. Acid-activated biochar increased sulfamethazine retention in soils.
568 *Environmental Science and Pollution Research*, **22**(3), 2175-2186.

569 40. Yaman, S. 2004. Pyrolysis of biomass to produce fuels and chemical feedstocks.
570 *Energy conversion and management*, **45**(5), 651-671.
571 41. Yao, Y., Gao, B., Inyang, M., Zimmerman, A.R., Cao, X., Pullammanappallil,
572 P., Yang, L. 2011. Removal of phosphate from aqueous solution by biochar
573 derived from anaerobically digested sugar beet tailings. *Journal of Hazardous*
574 *Materials*, **190**(1-3), 501-507.
575 42. Yu, X.-Y., Ying, G.-G., Kookana, R.S. 2009. Reduced plant uptake of pesticides
576 with biochar additions to soil. *Chemosphere*, **76**(5), 665-671.
577 43. Yuan, J.-H., Xu, R.-K., Zhang, H. 2011. The forms of alkalis in the biochar
578 produced from crop residues at different temperatures. *Bioresource Technology*,
579 **102**(3), 3488-3497.
580 44. Zelazny, L.W., He, L., Vanwormhoudt, A. 1996. Charge analysis of soils and
581 anion exchange. *Methods of Soil Analysis Part 3—Chemical*
582 *Methods*(methodsofsoilan3), 1231-1253.
583 45. Zhang, G., Zhang, Q., Sun, K., Liu, X., Zheng, W., Zhao, Y. 2011. Sorption of
584 simazine to corn straw biochars prepared at different pyrolytic temperatures.
585 *Environmental Pollution*, **159**(10), 2594-2601.
586 46. Zhang, M., Gao, B., Yao, Y., Xue, Y., Inyang, M. 2012. Synthesis,
587 characterization, and environmental implications of graphene-coated biochar.
588 *Science of the Total Environment*, **435-436**, 567-572.

589
590
591
592

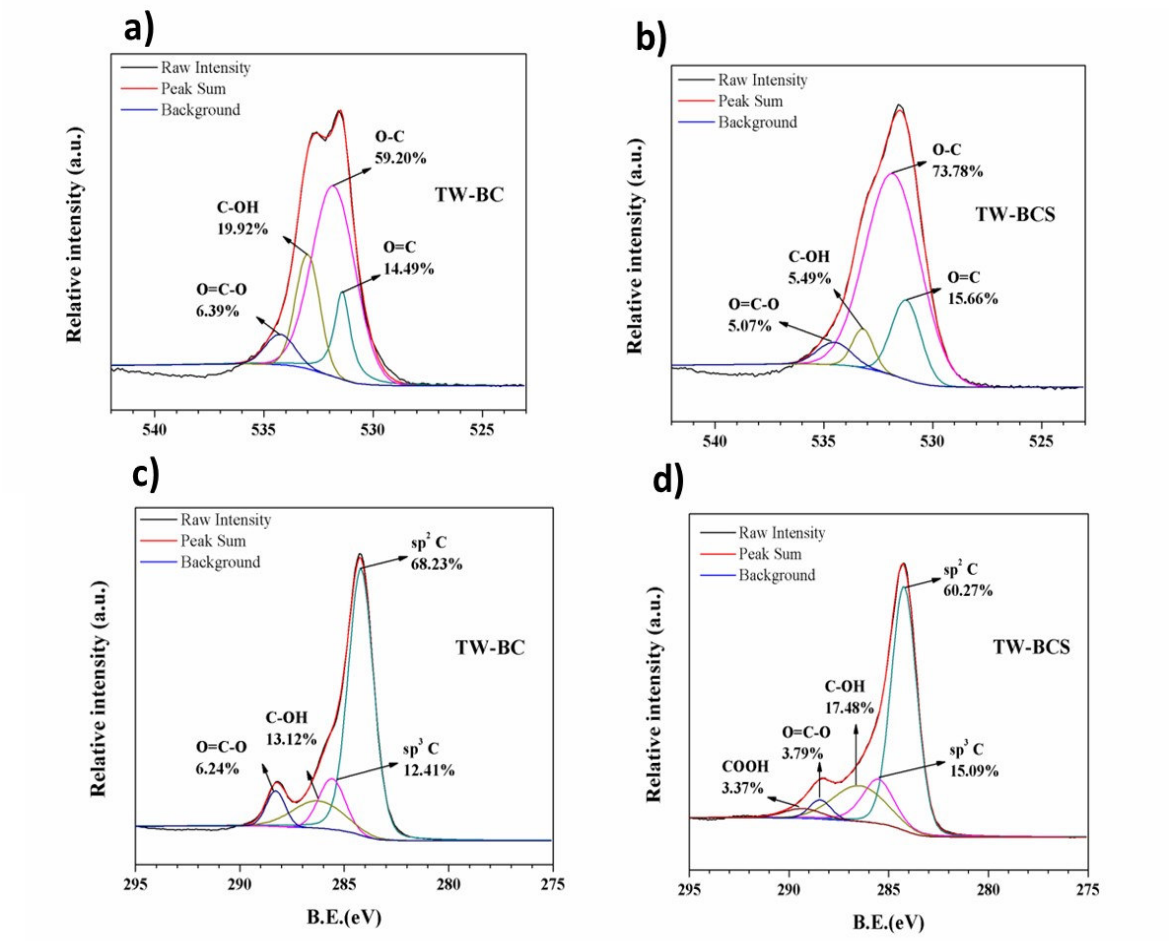

Figure 1: X-ray photoelectron spectroscopy (XPS) spectra of biochar samples: (a) O1 spectra for TW-BC, (b) O1 spectra for TW-BCS, (c) C1s spectra for TW-BC, and (d) C1s spectra for TW-BCS

TW-BC: Tea waste biochar; TW-BCS: Steam activated tea waste biochar

606

607

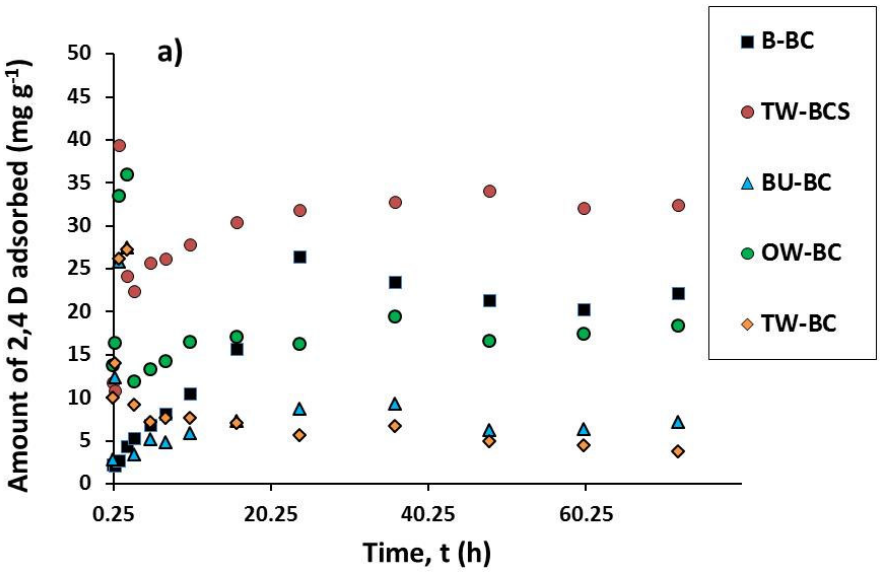

608

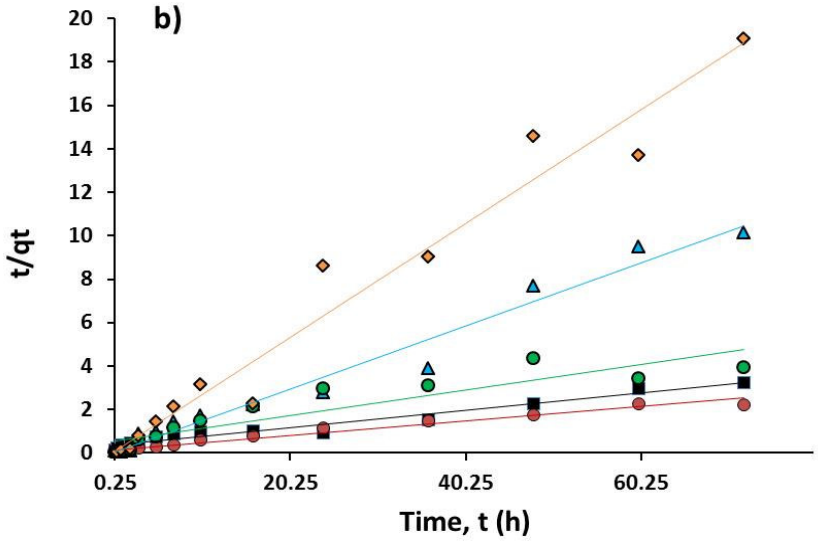

609

610 Figure 2: 2,4-D sorption kinetics on tea waste biochar (TW-BC), steam activated steam
611 waste biochar (TW-BCS), burcucumber biochar (BU-BC), oak wood biochar (OW-BC)
612 and bamboo biochar (B-BC) (a) sorption data; (b) amount of 2,4-D sorbed at time t
613 (t/qt) (pseudo-second order kinetic model fitting)

614

615

616

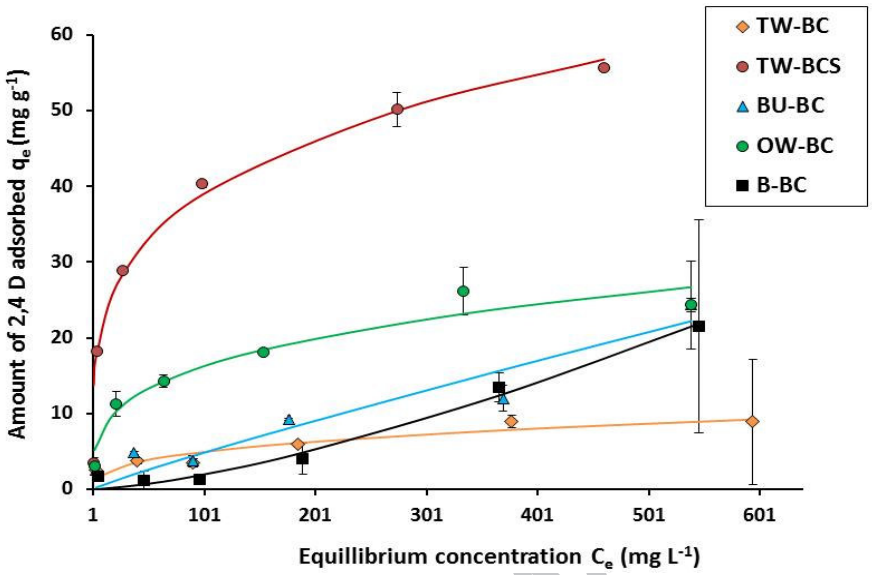

617

618 Figure 3: 2,4-D sorption isotherms on tea waste biochar (TW-BC), steam activated
619 steam waste biochar (TW-BCS), burcucumber biochar (BU-BC), oak wood biochar
620 (OW-BC) and bamboo biochar (B-BC) with Freundlich model fitting. Error bars
621 represent the standard deviation

622

623

Table 1: Physicochemical properties of five different biochar samples. Pore diameter and pore volume data were collected from Rajapaksha et al. (2014) and Vithanage et al. (2015)

Sample name	**Pyrolysis temperature (˚C)**	**pH**	**EC (µS m^{-1})**	**CEC ($cmol_c$ kg^{-1})**	**C%**	**N%**	**Surface area (m^2 g^{-1})**	**Pore volume (cm^3 kg^{-1})**	**Pore diameter (nm)**
TW-BC	700	10.8±0.06	62.7±0.35	2.3±0.15	72.8±0.25	3.7±0.09	421.3	57.6	1.9
TW-BCS	700	11.9±0.02	221.4±0.25	15.9±1.16	63.4±0.73	3.4±0.07	576.1	109.1	2.0
BU-BC	700	10.7±0.12	1403.3±0.21	2.5±5.29	43.8±0.19	3.2±0.01	2.3	8.4	0.7
OW-BC	400	10.4±0.22	73.7±0.31	2.6±0.31	84.3±0.57	0.8±0.03	270.7	120.0	1.1
B-BC	400	10.2±0.23	24.9±0.41	3.6±0.75	86.2±0.12	0.6±0.03	475.6	209.0	1.1

TW-BC: Tea waste biochar; TW-BCS: Steam activated tea waste biochar; BU-BC: Burcucumber biochar; OW-BC: Oak wood biochar; B-BC: Bamboo biochar; EC: Electrical conductivity; CEC: Cation exchange capacity; ± indicates the standard deviation (STD) values

632 Table 2: Fitted parameters values of sorption kinetic model (Pseudo-second order
633 model)

Biochar	**Pseudo-second order model parameters**		
	Q_t Amount of 2,4-D adsorbed at time t (mg g^{-1} min^{-1})	K_2 (sorption constant)	R^2
TW-BCS	71.50	0.21	0.96
TW-BC	50.42	0.04	0.99
BU-BC	27.62	0.09	0.98
OW-BC	39.52	0.02	0.95
B-BC	2.68	0.17	0.96

634 *TW-BC: Tea waste biochar, TW-BCS: Steam activated tea waste biochar, BU-BC:*
635 *Burcucumber biochar, OW-BC: Oak wood biochar, and B-BC: Bamboo biochar;*
636 *Kinetic models are presented in the supplementary information*

637

638

639

640

641

642

643

644

Table 3. Freundlich and Langmuir model parameters for sorption isotherm of 2,4-D on biochar

Biochar	**Freundlich model parameter**		
	K (sorption constant)	N (slope of sorption isotherm)	R^2
TW-BC	3.52	0.06	0.98
TW-BCS	3.63	0.75	0.98
BU-BC	0.22	0.30	0.85
OW-BC	2.23	0.39	0.94
B-BC	0.08	0.21	0.76
Biochar	**Langmuir model parameter**		
	K_f (sorption constant)	Q (maximum sorption capacity mg g^{-1})	R^2
TW-BC	0.02	10.05	0.96
TW-BCS	0.01	58.85	0.97
BU-BC	0.02	42.67	0.74
OW-BC	0.02	26.66	0.90
B-BC	0.04	28.92	0.71

TW-BC: Tea waste biochar, TW-BCS: Steam activated TW-BC, BU-BC: Burcucumber biochar, OW-BC: Oak wood biochar, B-BC: Bamboo biochar. Isotherm models are expressed in the supplementary information

Table 4: Distribution sorption coefficient (K_d and K_{oc}) of 2,4-D sorption for biochar samples

Biochar sample	**K_d (L kg^{-1})**	**K_{oc} (L kg^{-1})**
TW-BC	148.27	203.67
TW-BCS	1452.51	2291.02
BU-BC	155.72	355.53
OW-BC	404.68	480.05
B-BC	73.70	157.17

Tea waste biochar (TW-BC), steam activated tea waste biochar (TW-BCS), burcucumber biochar (BU-BC), oak wood biochar (OW-BC), and bamboo biochar (B-BC)

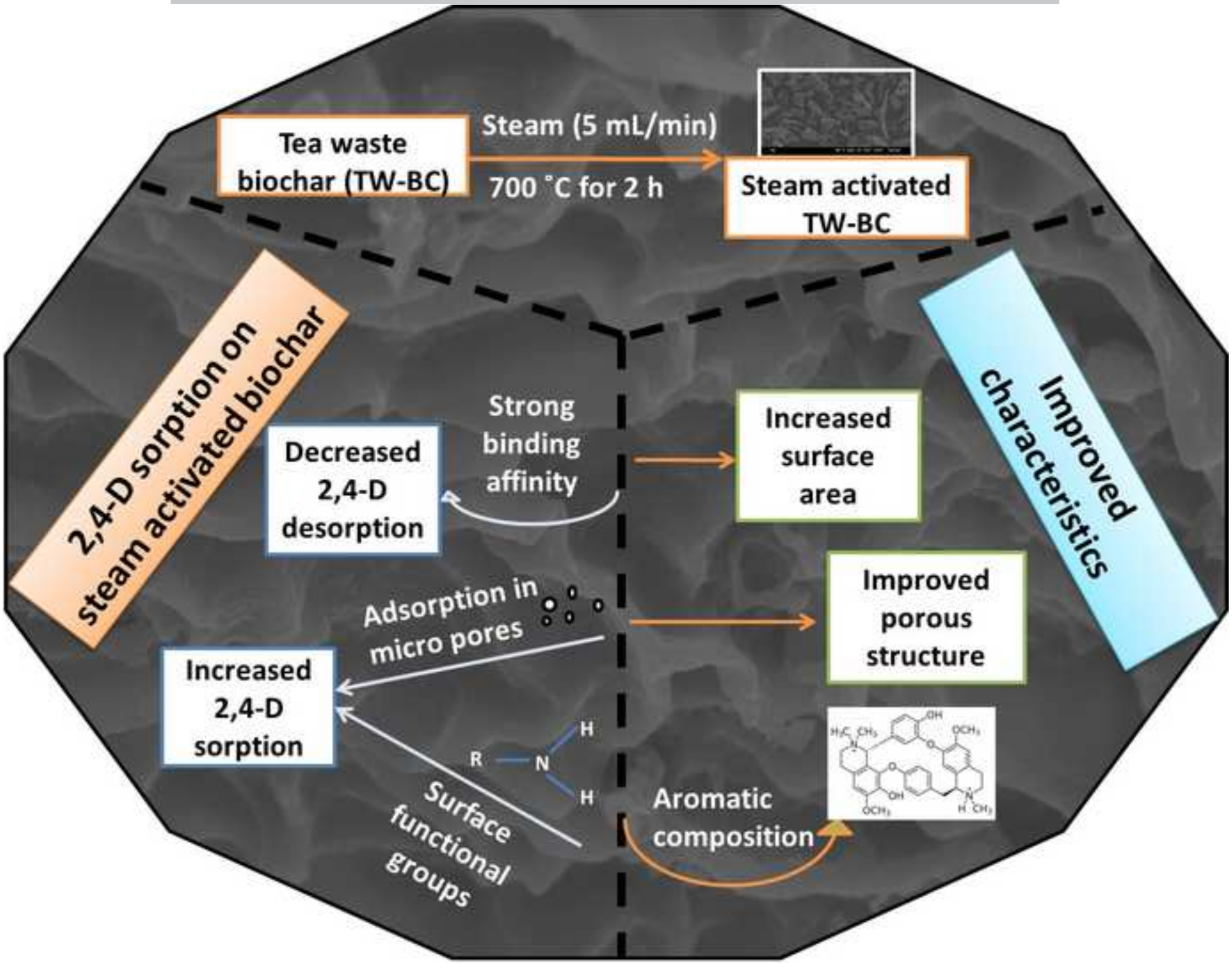

Highlights

1. Steam activated tea waste biochar sorbed the highest amount of 2,4-D
2. Steam activation increased biochar surface area and conserved oxygen-containing functional groups
3. 2,4-D desorption was lowest in steam activated biochar